THE JOURNAL OF PHYSICAL CHEMISTRY B

Article

pubs.acs.org/JPCB

Stimulus-Responsive Supramolecular pK_a Tuning of Cucurbit[7]uril Encapsulated Coumarin 6 Dye

Nilotpal Barooah, Jyotirmayee Mohanty, Haridas Pal, and Achikanath C. Bhasikuttan*

Radiation & Photochemistry Division, Bhabha Atomic Research Centre, Mumbai 400 085, India

Supporting Information

ABSTRACT: This article reports an efficient host-assisted guest protonation mechanism in coumarin 6 (C6) dye, upon its interaction with cucurbit[7]uril (CB7) macrocycle. C6 uptakes the CB7 macrocycle both in 1:1 and 2:1 (CB7/C6) stoichiometries, which brings out a large upward pK_a shift (from ~0.8 to 6), and facilitates the protonation of C6 at normal pH conditions, having significant photochemical implications. Controlled dissociation of the assemblies has been achieved through their response to stimuli like temperature change or metal ions. By this approach, a specific form of the guest can be activated and could provide a simple stimulus for the controlled drug/dye delivery. Furthermore, the host-assisted guest protonation improves the stability and aqueous solubility of C6 and is a promising candidate for aqueous-based supramolecular dye laser system. Such simple protocol leading to photoswitchable systems having aqueous solubility and biocompatibility can in principle be evolved into a general strategy to deliver and operate potential functional molecular components under various trigger control.

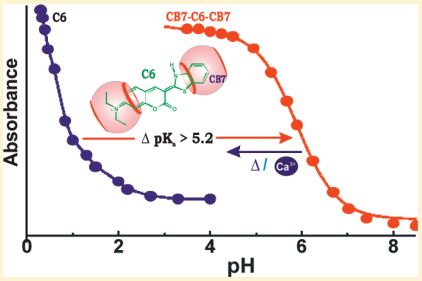

INTRODUCTION

The attributes of molecular self-assemblies and their distinct applications in chemistry,[1,2] biology,[3] and material science[1−4] have been growing dramatically in the recent years and is regarded as one of the major strategies for the nanolevel fabrication of functional molecular devices.[1−4] In this regard, the use of noncovalent interactions through supramolecular assembly of macrocyclic host and guest has received considerable research attention as they deliver pronounced modulations in the guest molecular properties.[1,5,6] Since the initial reports of guest binding by synthetic supramolecular assemblies, the complexity of structures, the reactivities, and the applications of host−guest systems have increased enormously. Presently, this approach has proved its utility in a wide range of applications such as in chemosensing,[7] optoelectronics like optical sensor,[8] on−off switches[9] and logic gates,[10] photostabilization,[11,12] supramolecular catalysis,[13,14] drug delivery vehicles,[15,16] enzymatic assay,[17] nanocapsules,[18] supramolecular architectures,[4,9,19] and other stimulus responsive functional devices.[20]

Among the vast repertoire of classical macrocyclic host molecules like cyclodextrins, calixarenes, crown ethers, etc., the cucurbiturils, e.g., cucurbit[7]uril (CB7, Chart 1) in particular, are versatile water-soluble receptor molecules consisting of methylene bridged glycoluril units having pumpkin shaped macrocyclic cavities (Chart 1).[6,21] Because of its unique structural features, cucurbiturils are capable of imparting both ion-dipole and hydrophobic interactions toward its guests, leading to strong and stable host−guest complexes. CBs have gained immense research interest because of their ability to host in a highly selective manner certain types of guest molecules such as small organic dyes through hydrophobic interaction,[6,21] metal cations and metal nanoparticles,[6,21,22] protonated alkyl and aryl amines,[23−25] and cationic dyes such as rhodamines,[11,12,26] triphenylmethane dyes,[27] and thioflavin T,[18,24,28,29] mainly through ion−dipole interaction. On the guest side, fluorogenic guests or its functionally-linked multichromophoric systems often respond beneficially on interaction with macrocyclic hosts, explicitly due to their positioning and stoichiometric composition with the host cavity. Among several potential coumarin dyes, derivatives like the bichromophoric coumarin 6 (C6, Chart 1) were projected as environment sensitive solvatochromic fluorophores suitable for in vivo imaging of cells in living organisms.[30]

Coumarin dyes have enjoyed much research interest in different areas due to their wide applicability and probably constitute one of the most thoroughly investigated systems by

Chart 1. Structures of Coumarin 6 and Cucurbit[7]uril

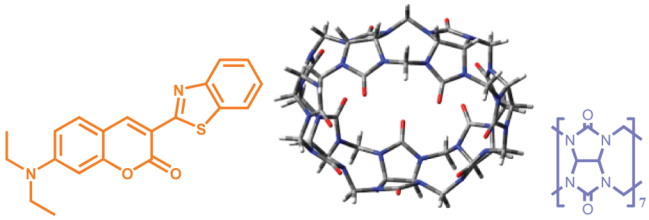

Received: December 25, 2011
Revised: February 28, 2012
Published: March 2, 2012

photophysicists.[31−33] Coumarin dyes form an active class of laser dyes[34,35] and have been explored extensively for its applications in biological systems,[30,36] stereoselective photodimerization,[37,38] etc. It has been shown that in heterogeneous supramolecular system like zeolites, C6 shows remarkable sensitivity for detecting the small amount of Lewis and Bronsted sites in the faujasite zeolite as well as in silica gel.[39] While in C6, the planarity and the electron density contribution from the $-NEt_2$ group toward the parent coumarin itself is an intriguing study of intramolecular charge transfer (ICT) or twisted intramolecular charge transfer (TICT) process in the excited state,[31] a macrocyclic interaction at the coumarin end is certainly expected to affect the charge distribution processes, which are expected to modulate its protolytic equilibrium favorably, promising tunable change in its chemical properties. Positively, the cucurbituril macrocycles do display differential affinity for the protonated and neutral forms of the guest, which makes the host−guest binding strongly pH sensitive, in other words, a resultant pK_a shift.

A number of reports have documented chemists' approaches in mimicking such pK_a shifts using macrocyclic interactions.[40−43] Pertinently, utilizing the inclusion property of CB7, complexation-induced pK_a shifts are conceptualized recently both in ground and excited states, which are extensively exploited toward the design of novel functional supramolecular systems.[7,8,10,42−44] More recently, following a host induced pK_a shift, Nau et al. have demonstrated the design of supramolecular logic with complexation of cucurbiturils as a supramolecular input.[10] A striking observation has recently been reported by Pluth et al., where the authors demonstrate the possibility to perform acid catalysis in a supramolecular host under alkaline conditions, owing to its ability to protonate an included guest.[13] They have also demonstrated that the driving forces for guest encapsulation dramatically alter the effective basicities of certain encapsulated amines up to 4.5 pK_a units.[45]

One of the major advantages in employing a noncovalent host−guest approach is their effective and quantitative response to external stimuli, such as light, environment, and exogenous ligands,[18,20,28,46] and have been well exploited for drug carrier/delivery,[20,44] sensing,[7] or enzymatic activity/assay.[3,17] In an earlier work, on the basis of the supramolecular pK_a shift and its metal ion response in neutral red dye on binding with CB7, we have demonstrated the salt-induced relocation of the dye from the macrocyclic cavity of CB7 into the biomolecular pocket of bovine serum albumin.[44] Influencing the proton transfer interactions in hydroxyphenyl benzimidazole, control over the excited state proton transfer (ESPT) reaction has been achieved through its CB7 encapsulation.[42] In the present case, the selected bichromophoric C6 is an interesting system for a coupled charge transfer and protolytic equilibrium, which reserve much of its photochemistry to extremely low pH conditions (below pH 1.0). Herein, we report host-assisted guest protonation of C6 using CB7 macrocycle, leading to an unprecedented supramolecular upward pK_a shift of ∼5.2 units, which has been judiciously tuned by temperature or metal ions as external stimuli. The highly fluorescent photoswitchable system provide access to the photochemistry of protonated C6 at normal pH conditions and improves its aqueous solubility (by ∼250 times), emphasizing its projected water-based applications.

EXPERIMENTAL SECTION

3-(2-Benzothiazolyl)-7-(diethylamino) coumarin (Coumarin 6 (C6)) and $CaCl_2$ were obtained from Sigma-Aldrich and were used as received. Coumarin 1 (C1) was obtained from Exciton. Ethanol (spectroscopic grade) was purchased from Merck India Ltd. Cucurbit[7]uril was synthesized according to a previously reported procedure and were characterized by ^{1}H NMR spectroscopy.[47] β-Cyclodextrin was from TCI, Japan. Nanopure water (Millipore Gradient A10 System; conductivity of 0.06 μS cm^{-1}) was used to prepare the sample solutions. $HCl/HClO_4$ as well as NaOH used for pH adjustment were obtained from Merck India. Solution pHs were measured by a pH meter model CL46+ from Toshcon Industries Ltd., India. Before measurements, the pH meter was calibrated at two pHs, namely, at pH 7 and pH 4, by using standard pH buffer solutions from Merck (India).

Ground state optical absorption spectra were recorded in 10 mm quartz cells using a Shimadzu model 160A UV−vis spectrophotometer (Tokyo, Japan). Steady-state fluorescence spectra were recorded using a Hitachi (Tokyo, Japan) model F-4500 spectrofluorimeter. Since C6 was sparingly soluble in water at pH ≈ 4.5, for optical absorption and emission measurements, ∼10 μL of stock solution of C6 in ethanol was added to 2 mL of nanopure water and stirred vigorously. This solution was further diluted with water and was used for optical measurements. The samples were excited at 465 nm to maintain minimum change in the absorbance in the presence of host and the small changes if any, have been corrected. Fluorescence quantum yields were measured by taking the reported value of C6 itself as standard (Φ_f (30% ethanol−water/H^+) = 0.1).[48] Time-resolved fluorescence measurements were carried out using a time-correlated-single-photon-counting (TCSPC) spectrometer (IBH, UK). In the present work, 445 nm diode laser (∼100 ps, 1 MHz repetition rate) was used as the excitation source and a microchannel plate photomultiplier tube (MCP PMT) was used for fluorescence detection. A reconvolution procedure was used to analyze the observed decays using a proper instrument response function obtained by substituting the sample cell with a light scatterer (suspension of TiO_2 in water). With the present setup, the instrument time resolution is adjudged to be better than 40 ps following reconvolution analysis. The fluorescence decays were analyzed as a sum of exponentials as[49,50]

$$I(t) = \sum_i B_i \exp(-t/\tau_i) \quad (1)$$

where, $I(t)$ is the time dependent fluorescence intensity, and B_i and τ_i are the pre-exponential factor and the fluorescence lifetime for the i^{th} component of the fluorescence decay, respectively. The quality of the fits and consequently the mono- or biexponential nature of the decays were judged by the reduced chi-square (χ^2) values and the distribution of the weighted residuals among the data channels.[49,50] For a good fit, the χ^2 value was close to unity, and the weighted residuals were distributed randomly among the data channels.[49,50] The ^{1}H NMR experiments were performed in D_2O (99.8%) using a Bruker Avance Ultrashield 700 MHz spectrometer at TIFR, Mumbai, India. For NMR spectroscopy, calculated amounts of C6 and CB7 were put together in a 2 mL microcentrifuge tube followed by the addition of D_2O. The solution was stirred for 1 h and centrifuged to remove any insoluble residues. Geometry optimization calculations were performed with the

dx.doi.org/10.1021/jp212459r | J. Phys. Chem. B 2012, 116, 3683−3689

Gaussian92 suite package at the PM3(MM) level, without any solvent consideration.[51]

RESULTS AND DISCUSSION

Absorption and Fluorescence Spectral Measurements. In aqueous solution containing <1% ethanol, C6 displayed a characteristic broad absorption band with maximum at 460 nm, having prominent shoulder bands as presented in Figure 1A.[48] As the pK_a of C6 is reported to be <1,[48] for the present experiments, the solution pH was set at ~4.5, exclusively to study the interaction of CB7 with the neutral form of the dye, C6. During the initial addition of CB7 (up to ~100 μM) to the C6 solution set at pH 4.5, the absorption band of C6 gradually became narrow with a decrease in the absorbance mainly in the blue side of the spectrum (Figure 1A). However, with further additions of CB7 to about 3 mM, a red-shifted band developed progressively, and the absorption maximum shifted ~61 nm bathochromically and transformed into a spectrally distinctive narrow and intense band, maintaining a clear isosbestic point at 470 nm as shown in Figure 1A. These spectral shifts clearly indicate a structural change of the absorbing chromophore, brought out by the cucurbituril encapsulation. Also, it may be mentioned here that though C6 is sparingly soluble in water, in the presence of CB7, the solubility of the dye increased by about 250 times (Note 1 and Figure S1, Supporting Information), which is an encouraging result in support of the aqueous-based applications of the dye.

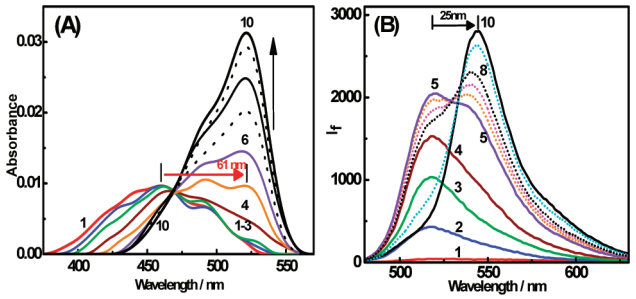

Figure 1. Absorption (A) and fluorescence (B) spectra of C6 (1.5 μM at pH 4.5) with [CB7]/mM: 0 (1); 0.025 (2); 0.050 (3); 0.10 (4); 0.25 (5); 0.35 (6); 0.45 (7); 0.58 (8); 1.2 (9); 3.0 (10). λ_{ex} = 470 nm.

In the emission front, though coumarin dyes are well-known for their applications as laser dyes,[34,35] in polar solvents, C6 exhibits very weak emission, which is centered at ca. 525 nm.[31] It is well established that *N,N′*-dialkyl substituted coumarin derivatives favor planar ICT states leading to a partially charged separated ground state, which in the excited state is highly liable to get transformed to a nonfluorescent TICT state. However, with the addition of CB7, the broad and weak fluorescence band intensified gradually with ~7 nm hypsochromic shift until the addition of ~100 μM of CB7 (Figure 1B). Thereafter, with increase in CB7 concentration, the emission intensity at the blue edge decreased considerably with concomitant development of a bathochromically shifted, distinct, and intense emission band having maximum at 545 nm as in Figure 1B. These changes in the emission properties, which corroborate the absorption spectral changes on the addition of CB7, reiterate the strong modulation in the molecular properties of C6 on interaction with CB7.

Considering molecular structure of C6, the presence of benzothiazole moiety is very important, as it is in conjugation with the electron donating $-NEt_2$ group at the coumarin end. An effective intramolecular charge transfer would make the thiazole nitrogen more electronegative and increases its proton affinity. As seen from the absorption and emission spectral changes provided in Figure S2, Supporting Information, this charge transfer stabilized and protonated C6 ($C6H^+$), displaying its characteristic spectral bands, which are bathochromically shifted from that of neutral C6. Note that these spectral changes closely resembled the changes seen during the titration of C6 with CB7 at pH 4.5 (Figure 1A). Thus, it is apparent that CB7−C6 interaction at pH 4.5, effectively brings out the molecular characteristics, which could otherwise be attained on protonation of C6.[48] This is an important observation and is a clear case of the host-assisted guest protonation process in the system.

Since both the coumarin and the benzothiazole moieties are prominent binding sites for CB7,[12,24] to understand the site and sequence of CB7 interaction, control experiments were performed with coumarin 1 dye (C1, Figure S3 inset, Supporting Information) in which the coumarin moiety has no benzothiazole unit attached. The absorption and fluorescence spectral changes in C1 on titration with CB7 have indicated only marginal spectral shifts (Figure S3, Supporting Information), which are attributed to the interactions of CB7 at the coumarin end. Hence, the dramatic red shift in C6 observed with higher CB7 concentration (~mM) also involves the interaction of CB7 at the benzothiazole end. The initial complexation of CB7 is thus driven by the ion−dipole interactions of partially positively charged $-NEt_2$ group with the negatively polarized carbonyl portal of CB7. This further stabilizes the ICT state and results in the emission enhancement observed in the blue side of the spectrum. However, the supramolecularly stabilized ICT state of the CB7−C6 complex (1:1), facilitates the protonation at the benzothiazole nitrogen, depending upon the solution pH. At pH 4.5, it is apparent that the proton concentration is insufficient for an immediate protonation reaction. However, when the CB7 concentration is increased to ~ 2 mM, the benzothiazole end of C6 also gets encapsulated by forming a 2:1 (2CB7/C6) complex, which further enhances the proton affinity of benzothiazole nitrogen and gets protonated to remain as $2CB7-C6H^+$ complex. This supramolecular stabilization of the protonated site makes the removal of H^+ extremely difficult and requires much stronger basic conditions, i.e., unusually large pK_a shift.

Cucurbit[7]uril Induced pK_a Shifts. With the protolytic equilibrium in focus, we evaluated the pK_a of C6 in solutions containing varying amounts of CB7 host. As shown in Figure 2,

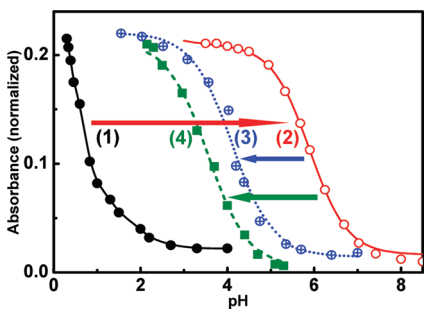

Figure 2. pH titrations of C6 (1.5 μM) in the absence of any additive (1) and in the presence of 3 mM CB7 (2); with 3 mM CB7 at 70 °C (3); with 3 mM CB7 and 50 mM $CaCl_2$ (4). The absorbance was measured at 520 nm.

dx.doi.org/10.1021/jp212459r | J. Phys. Chem. B 2012, 116, 3683−3689

in the absence of CB7, the absorbance changes in C6 (measured at 520 nm) with pH indicated a pK_a value of <0.8, which is in good agreement with the reported value.[48] It should be mentioned here that due to the very high acidic conditions required, we did not record the saturation of the $C6H^+$ absorption at very low pHs, and hence, the pK_a value 0.8 estimated here would be slightly on the higher side.[48] However, with the incremental addition of CB7, the pK_a curves showed a gradual upward shift (Figure 2; Figure S4, Supporting Information) and remained unchanged at pK_a ≈ 6 on using ca. 3 mM CB7. The large pK_a shift validates the presence of protonated C6 even at pH ≈ 4.5 in a C6 solution containing millimolar concentrations of CB7 host. Moreover, the fluorescence quantum yield of $C6H^+$ increased substantially from 0.08 in the absence of CB7 (at pH ≈ 0.5), to ∼0.74 in the presence of CB7, even in solution with pH 4.5. This manifests the retardation of the nonradiative relaxation channels, such as the TICT or intramolecular torsional motions, due to the rigid binding environment provided by the CB7 moieties at either ends of C6.

Considering the various protolytic equilibria feasible in the CB7−C6 solution with pH, the pK_a curves of Figures 2 and S4, Supporting Information, were fitted in accordance to a four-state equilibrium model[40,41] as described in Note 2, Supporting Information. The curve fitting analysis provided the pK_a values for C6 in presence of 0.1 mM, 0.6 mM, and 3 mM of CB7 as ∼1.9, 4, and 6, respectively. Since the pK_a of C6 in the absence of CB7 considered here is on the upper limit (0.8), we adjudge the supramolecular pK_a shift for the C6 dye in the presence of CB7 as large as >5.2 units, the largest host-assisted guest pK_a shift so far reported for a dye in a macrocyclic complex. Earlier Pluth et al. and Nau et al. have provided impressive examples of pK_a shifts by macromolecular hosts, with shifts up to 4.5 pK_a units.[16,45] Significance of the CB7−C6 binding is better realized when the above data are compared with the results of the β-cyclodextrin (βCD)−C6 interaction.[52] The titration measurements at pH 4.5 did not indicate any spectral band attributable to the protonated C6 even up to 10 mM βCD (Figure S5A, Supporting Information), clearly differentiating it from the interaction with the CB7 host.

Stoichiometric Composition and Binding Constants. From the pK_a curves in Figure 2, it is evident that at an alkaline pH (say ∼8.5), the dye would exist in its neutral form (without protonation at the thiazole nitrogen) and the interaction of CB7 would be mainly at the coumarin end in a 1:1 stoichiometry. At pH ≈ 2.5 (C6−2.5 μM), with >500 μM of CB7 (see Figure S4, Supporting Information), the protonated dye gets stabilized in a 2:1 complex, having the CB7 hosts at both the ends of $C6H^+$, as indicated in the inset of Figure 4. Since the carbonyl portals of CB7 are also prone to protonation at much lower pH, (pK_a of CB7 ≈ 2.2),[53] we did not evaluate the binding of preformed $C6H^+$ with CB7, which required very low pH conditions. On the basis of the above information, the feasible complexation/protonation processes at different pH conditions can be schematically represented as follows:

$$\mathrm{CB7} + \mathrm{C6} \rightleftharpoons \mathrm{CB7.C6} \overset{\mathrm{H^+}}{\rightleftharpoons} \mathrm{CB7.C6H^+} \overset{\mathrm{CB7}}{\rightleftharpoons} (\mathrm{CB7})_2.\mathrm{C6H^+} \quad (\mathrm{pH\ 2.5}) \tag{2}$$

$$\mathrm{CB7} + \mathrm{C6} \rightleftharpoons \mathrm{CB7.C6} \overset{\mathrm{CB7}}{\rightleftharpoons} (\mathrm{CB7})_2.\mathrm{C6} \overset{\mathrm{H^+}}{\rightleftharpoons} (\mathrm{CB7})_2.\mathrm{C6H^+} \quad (\mathrm{pH\ 4.5}) \tag{3}$$

$$\mathrm{CB7} + \mathrm{C6} \rightleftharpoons \mathrm{CB7.C6} \tag{4}$$

Thus, in solutions set at pH 8.5 and 2.5, the spectral profiles appropriately displayed distinct features attributable to the 1:1 and 2:1 complex formations as presented in Figures S6 and S7, Supporting Information, respectively. The Job plot method too differentiated the stoichiometric change, which graphically indicated maxima at ca. 0.5 and ca. 0.66 mole fractions of CB7 at pH 8.5 and 2.5 (Figure S8, Supporting Information), in good support to 1:1 and 2:1 complexes, respectively.

To evaluate the binding constants for the CB7−C6 interaction, the changes in the fluorescence intensities have been followed at preset pH conditions, 2.5 and 8.5, because of reasons discussed above. At pH 2.5, the 1:1 complex formation and the protonation are expected to be very fast, and the fluorescence intensity changes with an increase in CB7 can be conveniently considered as that of formation of 2:1 complex. For this, a modified Benesi−Hildebrand method[19] was attempted as discussed in Note 3, Supporting Information. Following this and analyzing the data as in Figure S9A, Supporting Information, the overall binding constant (K) value for the 2:1 stoichiometry was evaluated to be $\sim 1.5 \times 10^8$ M^{-2}. However, at pH 8.5, the interaction is only 1:1 complex formation and from the fluorescence changes (Figure S9B, Supporting Information), the binding constant was evaluated to be $(2.0 \pm 0.1) \times 10^3$ M^{-1} in accordance to a 1:1 complexation model.[40,54] However, similar analysis on the fluorescence titration data from the βCD−C6 system (Figure S5B, Supporting Information) at pH 4.5 provided the binding constant as $\sim 3 \times 10^2$ M^{-1}. The geometry optimization studies carried out at the PM3 (MM) level indicated that in both the cases of 1:1 and 2:1 stoichiometries claimed here, the optimized structures are well stabilized by the strong ion−dipole as well as hydrogen bonding interactions (Figure S10, Supporting Information). The protonated structures provided stable and planar geometrical arrangements having ΔH_f as −20 kcal/mol and −25 kcal/mol for the 1:1 and the 2:1 arrangements, respectively.

Excited State Lifetime and Anisotropy Measurements. The fluorescence decay profiles of C6 were recorded by a time correlated single photon counting (TCSPC) setup both in the absence and presence of CB7 at different pH conditions at their respective emission maxima. As displayed in Figure 3, the traces recorded from solutions at pH ≈ 0.5 (trace 1)

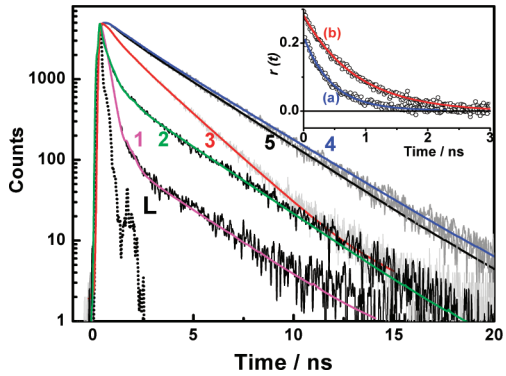

Figure 3. Fluorescence decay traces of C6 (∼1.5 μM) and CB7−C6 complexes at different pH conditions: C6 alone at pH 0.5 (1); pH 2.5 (2). C6 at pH 2.5, CB7 (200 μM) (3). C6 at pH 8.5, CB7 (3 mM) (4). C6 at pH 4.5, CB7 (100 μM) (5). λ_{ex} = 445 nm, λ_{mon} 550 nm. L represents the excitation lamp profile. The fitted (solid lines) values are given in Table S1, Supporting Information. Inset: Anisotropy decay traces for the CB7−C6 complex at pH 8.5 (a) and 2.5 (b).

dx.doi.org/10.1021/jp212459r | J. Phys. Chem. B 2012, 116, 3683−3689

and 2.5 (trace 2) provided the decay profiles having multi-exponential time constants with faster and slower components, due to the presence of protonated C6. The lifetime values obtained from suitable curve fitting as per eq 1 are provided in Table S1, Supporting Information. In the presence of CB7 at the respective pH conditions for the 2:1 and 1:1 stoichiometries (pH 2.5 and 8.5, respectively), the excited-state lifetimes increased substantially. This is expected due to severe retardation in the nonradiative torsional relaxation channels of C6 on CB7 encapsulation. The 1:1 complexes formed at pH 8.5 (trace 4) or at pH 4.5 with lower CB7 concentration (trace 5) displayed comparable decay profiles, whereas the decay trace corresponding to the 2:1 complex at pH 2.5 (trace 3) displayed a faster decay, contrary to that expected from its more rigid environment. This is understood as due to the strong hydrogen bonding interactions involved in the assembly, which contribute largely to the nonradiative processes.[55] In addition, the proposed stoichiometries are expected to exhibit a difference in the molecular hydrodynamic volumes, which in turn affect the rotational correlation times (τ_r) of C6.[40,54] At both the pHs, the anisotropy decays appeared single exponential (Note 4, Supporting Information, and Figure 3) with the decay at pH 8.5 significantly faster (τ_r = 485 ± 30 ps) compared to the decay at pH 2.5 (τ_r = 860 ± 40 ps). These τ_r values correspond to the diameters of ~15.5 Å and 20 Å, which are in good match for 1:1 and 2:1 complexes, respectively.

^{1}H NMR Measurements. The CB7−C6 interactions were also studied by ^{1}H NMR spectroscopy. Because of the inherent insolubility of C6 in D_2O, extensive titration experiments could not be carried out; nevertheless, the spectrum for the protonated form could be recorded in a mixture of CD_3COOD(5%)−DCl (10%)−D_2O. As already stated, since the solubility of C6 dramatically increases in the presence of mM concentrations of CB7, the NMR spectrum for the 2:1 complex could be recorded and compared with that of the protonated form of C6 as in Figure 4.

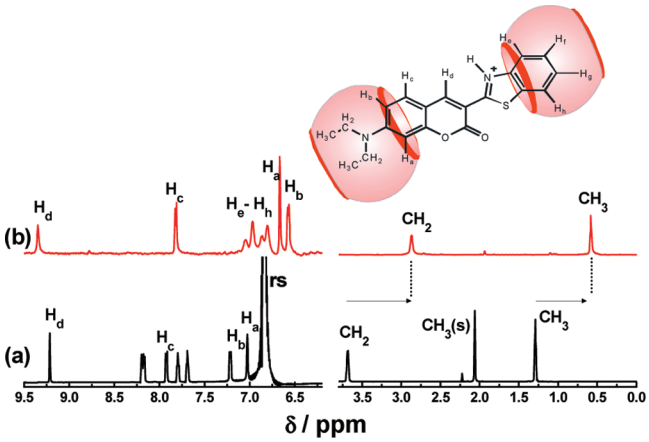

Figure 4. ^{1}H NMR spectra of C6 in D_2O at different environments: C6 in CD_3COOD (5%)−DCl (10%)−D_2O (a); C6 with 3 mM CB7 (b). Inset shows the pictorial representation of the CB7−C6 complex in a 2:1 stoichiometry.

In the presence of CB7, the methyl (δ 1.29) and the methylene (δ 3.67) protons of the $-N(Et)_2$ group show 0.7 and 0.8 ppm upfield shift indicating their complete inclusion inside the hydrophobic cavity of CB7. Concomitantly, the aromatic protons of the coumarin residue, namely, H_a (δ 7.03), H_b (δ 7.22), and H_c (δ 7.93), display 0.6 ppm, 0.3 ppm, and 0.1 ppm upfield shift, respectively. These upfield shifts in the presence of CB7 clearly demonstrate that they are embedded inside the CB7 cavity. In this 2:1 host−guest configuration, the effect of deshielding the carbonyl portal can be observed on the chemical shift of the coumarin proton H_d (δ 9.21), which instead shows an expected downfield shift of 0.24 ppm. In the 2:1 CB7−C6 stoichiometry, it is observed that the benzothiazole protons H_f/H_g (δ 7.69 and δ 7.80) and H_e/H_h (close spaced doublets at δ 8.16−8.19) show upfield shifts to the 6.75−7.1 ppm region and appear as broad unresolved signals. These observed changes demonstrate the complexation of C6 from both the ends by the CB7 hosts.

Thermal and Metal Ion Responsive pK_a Tuning. To take advantage of the large supramolecular pK_a shifts revealed in C6, stimulus responsive tuning has been attempted by simple stimuli such as temperature change or the addition of metal ions to affect the noncovalent interactions. On increasing the temperature, the intensity at the red-shifted absorption band in the 2:1 complex at pH 4.5 gradually decreased with concomitant blue shift of the spectrum, finally restoring the spectral features of a 1:1 stoichiometry, as shown in Figure 5A.

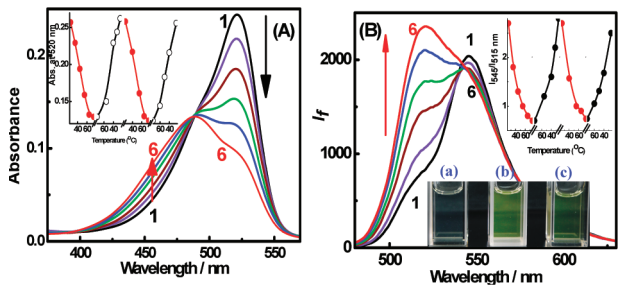

Figure 5. Absorption (A) and fluorescence (B) spectra of the 2:1 (CB7−C6) complex at pH 4.5 at temperatures (°C): 25 (1); 35 (2); 45 (3); 55 (4); 65 (5); and 75 (6). Inset A: absorbance at 520 nm plotted with temperature change. Inset B: ratio of the intensity changes at 545 and 515 nm plotted with temperature change. The picture shows the image of C6 solution (a); C6 with CB7 (b), and C6 with CB7 at 70 °C (c). λ_{ex} = 488 nm.

In other words, destabilization of the CB7 binding at the thiazole end takes place, thus shifting the equilibrium toward the 1:1 complex. In the emission measurements too (Figure 5B), the shoulder band at the blue side of the emission spectrum developed strongly to register an emission maximum at 520 nm, which corresponds to the 1:1 complex. The fact that we observed growth of the emission band on increasing the temperature suggests that there is no complete breakdown of the complex. In case of a complete dissociation, we expect very weak emission, which would be hardly visible, and the emission spectrum would show a decrease in intensity.

In the light of these stoichiometric changes, the pK_a curves for the 2:1 complex were evaluated at different temperatures, which displayed reversal of the pK_a shifts, demonstrating a thermo-responsive supramolecular pK_a tuning. The pK_a curve evaluated at a solution temperature of 70 °C is displayed in Figure 2, which provided the pK_a as 4.1. Further, the reversibility of the thermo-responsive tuning has also been established by performing repeated temperature change cycles, during which the absorbance changes at 520 nm remained reproducible as shown in the inset of Figure 5A. At the emission front also, the plot of intensity ratio at 545 and 515 nm displayed similar reversibility (Figure 5B inset). Visually,

dx.doi.org/10.1021/jp212459r | J. Phys. Chem. B 2012, 116, 3683−3689

the CB7−C6 solution on heating to ∼70 °C showed noticeable color change (Figure 5B inset), which acknowledge the thermo-responsive tuning mechanism established here.

Second, the addition of guests like metal ions as release stimulants has been attempted, which are expected to competitively bind at the CB7 portals, thus replacing the dye from the CB7 complex.[44] On addition of Ca^{2+} (up to ∼4 mM) to the 2:1 complex maintained at pH 4.5, the absorption and emission spectra gradually reversed (Figure S11, Supporting Information) similar to the case of temperature jump, manifesting the dissociation of CB7 from the thiazole end to give the 1:1 complex. However, interestingly, with higher concentrations of Ca^{2+} (0.1−2 M), the blue-shifted emitting species decreased in intensity concurrently indicating the complete disruption of the complex leaving behind the weakly emissive uncomplexed C6 in solution, even at pH 2.5 (Figure S12, Supporting Information). With varying concentration of Ca^{2+} ions, e.g., ∼10 mM and 50 mM, the evaluated pK_a curves provided the pK_a values as 4.2 and 3.5, respectively (Figure S4, Supporting Information). Thus, using different CB7 and Ca^{2+} concentrations, we propose to control the pK_a of C6, which is now tunable between 0.8 and 6.0.

The large dynamic range of the CB7 assisted pK_a shift and the corresponding emission yields, which are responsive to the solution temperature or the presence of metal ions find its utility for the construction of fluorescence on/off systems, or in other words, as molecular logics with CB7 as a supramolecular input. Our attempt to demonstrate some of the logic gates using the CB7−C6 system has been promising and are discussed in Note 5, Supporting Information (Figure S13 and Table S2). In general, such supramolecular photoswitchable systems, which can be triggered with simple stimuli like pH or temperature would find definite usage since a large number of tailor-made guest molecules can be activated based on these supramolecular interactions.

CONCLUSIONS

In conclusion, here we establish an efficient host-assisted guest protonation mechanism in a coumarin dye, C6, and demonstrate that a simple supramolecular interaction on part of a conjugated chemical system can greatly influence the stereo-electrotnics of a remote part, leading to considerable change in its chemical as well as photophysical characteristics. The documented supramolecular pK_a shift, which is more than 5.2 units accomplished in a macrocyclic complex, is novel and is attributed due to the supramolecular effect on the coupled intramolecular charge transfer and the protolytic equilibrium processes in C6. Also, for the first time, we demonstrate a convenient thermo-responsive pK_a tuning, in addition to the metal ion responsive tuning, which could act as a simple stimulus for the controlled dissociation of the complex, thus activating the protonated/deprotonated form of the guest. Since the stability and activity of dyes/drugs are often linked to their protonation state, the supramolecular encapsulation by CB7 and hence the control could provide an interesting tool to improve dye/drug stability, aqueous solubility, and drug release strategy through a host-assisted guest protonation. However, the CB7−C6 system could be a promising candidate for the aqueous-based supramolecular dye lasers,[35] which is being investigated in detail.

ASSOCIATED CONTENT

Supporting Information

Additional figures, tables and discussion. This material is available free of charge via the Internet at http://pubs.acs.org.

AUTHOR INFORMATION

Corresponding Author

*E-mail: bkac@barc.gov.in.

Notes

The authors declare no competing financial interest.

ACKNOWLEDGMENTS

We acknowledge the encouragement and support provided by Dr. S. K. Sarkar, Head, RPCD, and Dr. T. Mukherjee, Director, Chemistry group, BARC, during the studies.

REFERENCES

(1) Chen, Y.; Liu, Y. *Chem. Soc. Rev.* **2010**, *39*, 495−505.
(2) Raymo, F. M.; Stoddart, J. F. In *Molecular Switches*; Feringa, B. L., Ed.; Wiley-VCH: Weinheim, Germany, 2001; Vol. 7.
(3) Park, C.; Kim, H.; Kim, S.; Kim, C. *J. Am. Chem. Soc.* **2009**, 16614−16615.
(4) Frampton, M. J.; Anderson, H. L. *Angew. Chem., Int. Ed.* **2007**, *46*, 1028−1064.
(5) Arunkumar, E.; Forbes, C. C.; Smith, B. D. *Eur. J. Org. Chem.* **2005**, 4051−4059.
(6) Bhasikuttan, A. C.; Pal, H.; Mohanty, J. *Chem. Commun.* **2011**, *47*, 9959−9971.
(7) Bakirci, H.; Nau, W. M. *Adv. Funct. Mater.* **2006**, *16*, 237−242.
(8) Wang, R.; Yuan, L.; Macartney, D. H. *Chem. Commun.* **2005**, 5867−5869.
(9) Ko, Y. H.; Kim, E.; Hwang, I.; Kim, K. *Chem. Commun.* **2007**, 1305−1315.
(10) Pischel, U.; Uzunova, V. D.; Remon, P.; Nau, W. M. *Chem. Commun.* **2010**, *46*, 2635−2637.
(11) Mohanty, J.; Nau, W. M. *Angew. Chem., Int. Ed.* **2005**, *44*, 3750−3754.
(12) Nau, W. M.; Mohanty, J. *Int. J. Photoenergy* **2005**, *7*, 133−141.
(13) Pluth, M. D.; Bergman, R. G.; Raymond, K. N. *Science* **2007**, *316*, 85−88.
(14) Singleton, M. L.; Reibenspies, J. H.; Darensbourg, M. Y. *J. Am. Chem. Soc.* **2010**, 8870−8871.
(15) Jeon, Y. J.; Kim, S.-Y.; Ko, Y. H.; Sakamoto, S.; Yamaguchi, K.; Kim, K. *Org. Biomol. Chem.* **2005**, *3*, 2122−2125.
(16) Saleh, N.; Koner, A. L.; Nau, W. M. *Angew. Chem., Int. Ed.* **2008**, *47*, 5398−5401.
(17) Ghale, G.; Ramalingam, V.; Urbach, A. R.; Nau, W. M. *J. Am. Chem. Soc.* **2011**, *133*, 7528−7535.
(18) Dutta Choudhury, S.; Mohanty, J.; Pal, H.; Bhasikuttan, A. C. *J. Am. Chem. Soc.* **2010**, *132*, 1395−1401.
(19) Mohanty, J.; Bhasikuttan, A. C.; Dutta Choudhury, S.; Pal, H. *J. Phys. Chem. B* **2008**, *112*, 10782−10785.
(20) Angelos, S.; Yang, Y.-W.; Patel, K.; Stoddart, J. F.; Zin, J. I. *Angew. Chem., Int. Ed.* **2008**, *47*, 2222−2226.
(21) Lagona, J.; Mukhopadhyay, P.; Chakrabarti, S.; Isaacs, L. *Angew. Chem., Int. Ed.* **2005**, *44*, 4844−4870.
(22) Barooah, N.; Bhasikuttan, A. C.; Sudarsan, V.; Dutta Choudhury, S.; Pal, H.; Mohanty, J. *Chem. Commun.* **2011**, *47*, 9182−9184.
(23) Marquez, C.; Nau, W. M. *Angew. Chem., Int. Ed.* **2001**, *40*, 3155−3160.
(24) Dutta Choudhury, S.; Mohanty, J.; Upadhyaya, H. P.; Bhasikuttan, A. C.; Pal, H. *J. Phys. Chem. B* **2009**, *113*, 1891−1898.
(25) Shaikh, M.; Dutta Choudhury, S.; Mohanty, J.; Bhasikuttan, A. C.; Pal, H. *Phys. Chem. Chem. Phys.* **2010**, *12*, 7050−7055.

(26) Mohanty, J.; Jagtap, K.; Ray, A. K.; Nau, W. M.; Pal, H. *ChemPhysChem* **2010**, *11*, 3333−3338.
(27) Bhasikuttan, A. C.; Mohanty, J.; Nau, W. M.; Pal, H. *Angew. Chem., Int. Ed.* **2007**, *46*, 4120−4122.
(28) Mohanty, J.; Dutta Choudhury, S.; Upadhyaya, H. P.; Bhasikuttan, A. C.; Pal, H. *Chem.—Eur. J.* **2009**, *15*, 5215−5219.
(29) Bhasikuttan, A. C.; Dutta Choudhury, S.; Pal, H.; Mohanty, J. *Isr. J. Chem.* **2011**, *51*, 634−645.
(30) Signore, G.; Nifosi, R.; Albertazzi, L.; Storti, B.; Bizzarri, R. *J. Am. Chem. Soc.* **2010**, *132*, 1276−1288.
(31) Satpati, A. K.; Kumbhakar, M.; Maity, D. K.; Pal, H. *Chem. Phys. Lett.* **2005**, *407*, 114−118.
(32) Pinheiro, A. V.; Parola, A. J.; Baptista, P. V.; Lima, J. C. *J. Phys. Chem. A* **2010**, *114*, 12795−12803.
(33) Zhou, P.; Song, P.; Liu, J.; Han, K.; He, G. *Phys. Chem. Chem. Phys.* **2009**, *11*, 9440−9449.
(34) Anufrik, S. S.; Tarkovsky, V. V. *J. Appl. Spectrosc.* **2010**, *77*, 640−647.
(35) Azim, S. A.; Al-Hazmy, S. M.; Ebeid, E. M.; El-Daly, S. A. A *Opt. Laser Technol.* **2005**, *37*, 245−249.
(36) Madhavan, G. R.; Balraju, V.; Mallesham, B.; Chakrabarti, R.; Lohray, V. B. *Bioorg. Med. Chem. Lett.* **2003**, *13*, 2547−2551.
(37) Barooah, N.; Pemberton, B. C.; Sivaguru, J. *Org. Lett.* **2008**, *10*, 3339−3342.
(38) Pemberton, B. C.; Barooah, N.; Srivatsava, D. K.; Sivaguru, J. *Chem. Commun.* **2010**, *46*, 225−227.
(39) Corrent, S.; Hahn, P.; Pohlers, G.; Connolly, T. J.; Scaiano, J. C.; Fornes, V.; Garcia, H. *J. Phys. Chem. B* **1998**, *102*, 5852−5858.
(40) Mohanty, J.; Bhasikuttan, A. C.; Nau, W. M.; Pal, H. *J. Phys. Chem. B* **2006**, *110*, 5132−5138.
(41) Shaikh, M.; Mohanty, J.; Singh, P. K.; Nau, W. M.; Pal, H. *Photochem. Photobiol. Sci.* **2008**, *7*, 408−414.
(42) Shaikh, M.; Dutta Choudhury, S.; Mohanty, J.; Bhasikuttan, A. C.; Nau, W. M.; Pal, H. *Chem.—Eur. J.* **2009**, *15*, 12362−12370.
(43) Barooah, N.; Mohanty, J.; Pal, H.; Bhasikuttan, A. C. *Phys. Chem. Chem. Phys.* **2011**, *13*, 13117−13126.
(44) Shaikh, M.; Mohanty, J.; Bhasikuttan, A. C.; Uzunova, V. D.; Nau, W. M.; Pal, H. *Chem. Commun.* **2008**, 3681−3683.
(45) Pluth, M. D.; Bergman, R. G.; Raymond, K. N. *J. Am. Chem. Soc.* **2007**, *129*, 11459−11467.
(46) Rauwald, U.; Barrio, J.; Loh, X. J.; Scherman, O. A. *Chem. Commun.* **2011**, *47*, 6000−6002.
(47) Marquez, C.; Huang, F.; Nau, W. M. *IEEE Trans. Nanobiosci.* **2004**, *3*, 39−45.
(48) Jones, G. II; Jimenez, J. A. C. *Tetrahedron Lett.* **1999**, *40*, 8551−8555.
(49) Lakowicz, J. R. *Principles of Fluorescence Spectroscopy*, 3rd ed.; Springer: New York, 2006.
(50) O'Connor, D. V.; Phillips, D. *Time Correlated Single Photon Counting*; Academic Press: New York, 1984.
(51) Frisch, M. J.; Trucks, G. W.; Head-Gordon, M.; Gill, P. M. W.; Wong, M. W.; Foresman, J. B.; Johnson, B. G.; Schlegel, H. B.; Robb, M. A.; Replogle, E. S.; Gomperts, R.; Andres, J. L.; Raghavachari, K.; Binkley, J. S.; Gonzalez, C.; Martin, R. L.; Fox, D. J.; Defrees, D. J.; Baker, J.; Stewart, J. J. P.; Pople, J. A. *Gaussian 92*, revision E.01; Gaussian, Inc.: Pittsburgh, PA, 1992.
(52) Palcut, M.; Rabara, L. *Acta Chim. Slov.* **2009**, *56*, 845−851.
(53) Hwang, I.; Jeon, W. S.; Kim, H.-J.; Kim, D.; Kim, H.; Selvapalam, N.; Fujita, N.; Shinkai, S.; Kim, K. *Angew. Chem., Int. Ed.* **2007**, *46*, 210−213.
(54) Dutta Choudhury, S.; Mohanty, J.; Bhasikuttan, A. C.; Pal, H. *J. Phys. Chem. B* **2010**, *114*, 10717−10727.
(55) Cser, A.; Nagy, K.; Biczók, L. *Chem. Phys. Lett.* **2002**, *360*, 473−478.